# A Review of Power Electronics for Grid Connection of Utility-Scale Battery Energy Storage Systems

Wang, Guishi; Konstantinou, Georgios; Townsend, Christopher D.; Pou, Josep; Vazquez, Sergio; Demetriades, Georgios D.; Agelidis, Vassilios Georgios

2016

Wang, G., Konstantinou, G., Townsend, C. D., Pou, J., Vazquez, S., Demetriades, G. D., et al. (2016). A Review of Power Electronics for Grid Connection of Utility-Scale Battery Energy Storage Systems. IEEE Transactions on Sustainable Energy, 7(4), 1778-1790.

https://hdl.handle.net/10356/80331

https://doi.org/10.1109/TSTE.2016.2586941

# A Review of Power Electronics for Grid Connection of Utility-Scale Battery Energy Storage Systems

Guishi Wang, *Member, IEEE,* Georgios Konstantinou, *Member, IEEE,* Christopher D. Townsend, *Member, IEEE,*
Josep Pou, *Senior Member, IEEE,* Sergio Vazquez, *Senior Member, IEEE,*
Georgios D. Demetriades, *Member, IEEE,* and Vassilios G. Agelidis, *Fellow, IEEE*

***Abstract*—The increasing penetration of renewable energy sources (RES) poses a major challenge to the operation of the electricity grid owing to the intermittent nature of their power output. The ability of utility-scale battery energy storage systems (BESS) to provide grid support and smooth the output of RES in combination with their decrease in cost has fueled research interest in this technology over the last couple of years. Power electronics (PE) is the key enabling technology for connecting utility-scale BESS to the medium voltage grid. PE ensure energy is delivered while complying with grid codes and dispatch orders. Simultaneously, the PE must regulate the operating point of the batteries, thus for instance preventing overcharge of batteries. This paper presents a comprehensive review of PE topologies for utility BESS that have been proposed either within industry or the academic literature. Moreover, a comparison of the presently most commercially viable topologies is conducted in terms of estimated power conversion efficiency and relative cost.**

***Index Terms*—Battery energy storage system, dc-ac converter, dc-dc converter, power conversion, power electronics**

## I. Introduction

Renewable energy sources (RES), including wind turbines and solar PV systems, have been installed at a fast pace globally in recent years [1], [2]. The intermittent nature of output power from RES becomes a serious concern for the stability of the grid, particularly with increased RES penetration and at times when a high percentage of instantaneous demand is supplied by RES. In the case of Germany where 80% of instantaneous demand was supplied by RES on the 23$^{\text{rd}}$ August 2015 [3], significant operating reserves were required to meet the demand in case of a sudden decrease in the output of RES, thus causing an increase in the operational cost of the electricity network. Utility-scale battery energy storage systems (BESS) featuring fast response characteristics can provide an economic and promising alternative to smooth the output power of RES [4] and provide operating reserves [5], as there is virtually no cost to the system when BESS are in reserve state i.e. not providing power [6].

G. Wang, G. Konstantinou, and V.G. Agelidis are with the School of Electrical Engineering and Telecommunications, UNSW Australia, Sydney, NSW 2052, Australia (e-mail: allen.wang@unsw.edu.au, g.konstantinou@unsw.edu.au,vassilios.agelidis@unsw.edu.au).

C.D. Townsend is with the School of Electrical Engineering and Computer Science, University of Newcastle, Australia, (e-mail: townsend@ieee.org)

J. Pou is with the School of Electrical and Electronic Engineering, Nanyang Technological University, 639798 Singapore (e-mail: j.pou@ntu.edu.sg).

S. Vazquez is with the Electronic Engineering Department, Universidad de Sevilla, Sevilla, 41004, Spain, (e-mail: sergi@us.es).

G.D. Demetriades is with ABB Corporate Research,Vasteras, 72128, Sweden (e-mail: georgios.demetriades@se.sbb.com).

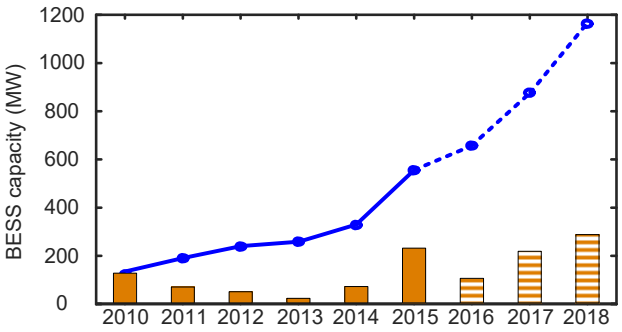


Fig. 1. Annual and cumulative installed capacity of utility-scale BESS (i.e. >10 MW) and their projected growth based on currently announced projects.

In general, BESS are capable of providing multiple market related and grid support services. For instance, besides providing operating reserves, BESS can be a potential alternative to peaking gas turbines [7]. In terms of grid support, fast response of BESS makes them suitable for providing frequency control as part of ancillary services [8]. In addition, BESS can help to black-start networks while providing voltage support for the transmission and/or distribution lines [8]. At the time of writing, numerous utility-scale BESS (i.e. > 10 MW) have been commissioned or announced in the world (59 projects according to DOE Global Energy Storage database [9]). The capacity of commissioned BESS has increased rapidly over the last couple of years with their growth expected to continue at a similar rate in the near future, as shown in Fig. 1.

Power electronics (PE) is the key enabling technology facilitating the connection of BESS rated at tens of MWs to the medium voltage (MV) electricity grid [10]–[15]. The PE unit serves as the interface between the batteries and the electricity grid, thus ensuring grid codes and standards are met when providing services to the market or the grid. Simultaneously, the PE unit controls the power flow of the BESS and regulates the operating points of the batteries, ensuring the life expectancy of BESS.

Owing to the growing popularity of BESS, many PE topologies have been proposed in the literature [10]–[12], [16]–[25]. The PE conversion system is desired to be as efficient as possible, as BESS are a lossy net energy consumer. However, PE topologies suitable for utility-scale BESS have not been thoroughly compared in the existing literature on the basis of performance and economic viability. This paper systematically

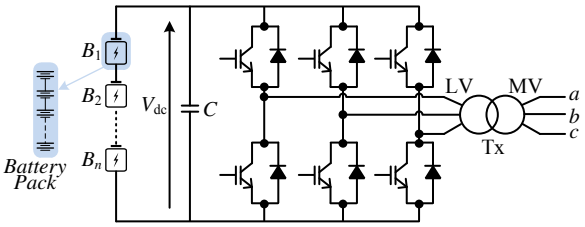


Fig. 2. Conventional PE unit using a 2L converter and transformer.

classifies PE topologies for utility BESS applications and reviews their application. Moreover, comparisons among the most commercially viable PE topologies are provided in terms of the estimated power conversion efficiency and relative cost.

The rest of this paper is organized as follows. PE topologies using line-frequency transformers are presented in Section II and transformerless topologies are reviewed in Section III. An analysis of the requirements for a dc-dc conversion stage is provided in Section IV. Section V introduces the required modifications of PE systems for hybrid energy storage systems (HESS). A comprehensive comparison among reviewed topologies is presented in Section VI. Finally, Section VII draws conclusions based on the presented comparison.

## II. Transformer Based PE Topologies

A conventional grid-connected PE unit for BESS applications consists of a simple two-level (2L) converter with a line frequency transformer (Tx) as shown in Fig. 2 [10], [26]. The transformer is used to boost the voltage from hundreds of volts to medium voltage (MV) levels, i.e., tens of kVs. Many batteries and their associated PE units can be connected in parallel at the low voltage dc bus to create large-scale BESS with power ratings at tens of MWs. Another transformer stage may be added for connection to a higher voltage level, i.e. 66 kV and above.

Alternative topologies to the well-established 2L converter, for BESS application, include the three-level (3L) neutral-point clamped (NPC) converter [27], [28], the active NPC (ANPC) converter, as shown in Fig. 3, and the 3L flying capacitor converter. A number of five-level converters have also been proposed [29]–[31]. The control design and modulation techniques for these converters are more complicated than the conventional 2L converter [23], [32], [33], however, they provide an extra degree of freedom to increase the output voltage magnitude of the converter and improve harmonic performance. There is a trade-off for different types of multi-level monolithic converters between the increased installed silicon power, the mechanical complexity and harmonic performance.

## III. Transformerless PE Topologies

The line-frequency transformer used in the previously described PE units is bulky, lossy and costly. To avoid the use of a line-frequency transformer, directly connected utility-scale BESS solutions have been developed. These solutions can be classified in two main categories: 1) those based on the series connection of semiconductors; 2) those based on the series connection of sub-modules (SMs).

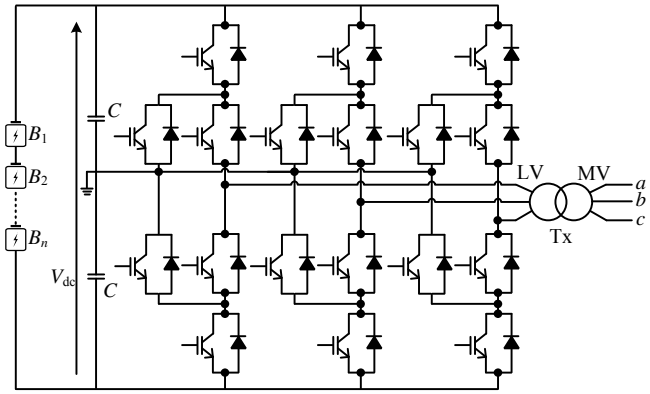


Fig. 3. Three-level active neutral-point clamped converter.

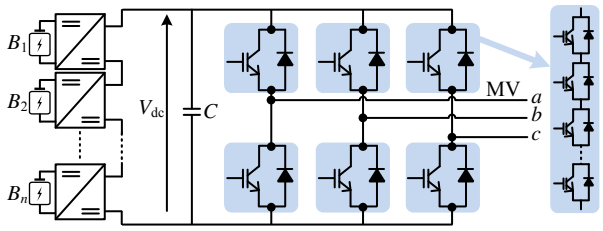


Fig. 4. Example of series connection of IGBTs for direct connection to medium voltage grid using a 2L converter.

### A. Series Connection of Semiconductors

For direct connection to the MV ac grid, many 2L or 3L converter topologies can still be utilized. An example using a 2L converter is presented in Fig. 4. Compared to Fig. 2, multiple IGBTs are connected in series, as a single IGBT with a voltage rating of a few kV (e.g. 1.7 kV - 6.5 kV) is unable to block the required dc-link voltage. However, some drawbacks of this approach include implications for the converters physical construction with many series-connected switching devices, and specific design of the gate driver / semiconductors to ensure each device is synchronously turned on/off. Use of this topology also necessitates a low switching frequency to achieve acceptable switching losses, which in turn implies higher cost of output filters, as will be explored in Section VI.

### B. Series Connection of Sub-modules

Direct connection of BESS to the MV grid without the use of a line-frequency transformer can be achieved through the use of cascaded modular converters based on a basic PE block (also referred to as bridge, submodule or cell) [34].

*1) Cascaded H-bridge Converter (CHB):* The CHB, as illustrated in Fig. 5, consists of three phase legs, each having multiple H-bridge cells connected in series [35]–[38]. The utility-scale BESS is normally composed of hundreds of battery modules. Therefore, battery modules can be equally distributed to each cell in the form of shorter battery strings [38], [39].

The use of cascaded topologies enables boosting each low voltage battery string to MV levels without the use of

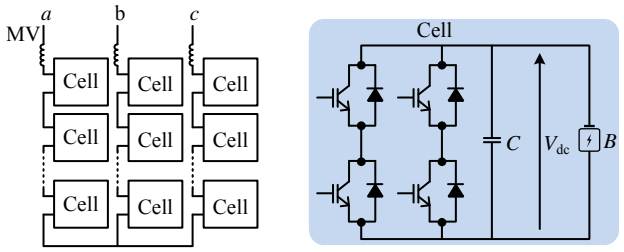


Fig. 5. Three-phase cascaded H-bridge converter and H-bridge cell.

transformers [19]. Each full bridge can regulate the power flow of the battery modules connected to its dc-link. A common zero-sequence voltage can be added to each phase-leg, thus enabling the transfer of energy between each phase-leg [40]–[43]. Advanced control algorithms have been proposed to deal with the issue of state of charge (SOC) unbalance within utility-scale BESS using the CHB converters [19], [20], [37], [38], [44], [45].

*2) Modular Multilevel Converter (MMC):* The MMC topology with half-bridge sub-modules (Fig. 6) provides an alternative cascaded topology for the integration of utility-scale BESS and has attracted research interest over recent years [18], [46]–[51]. The structure of the MMC allows for connection of the energy storage elements either directly to the MV dc-link or in a distributed manner across the sub-modules that form the converters arms [18], [46], [51], [52]. In the case of centralized batteries connected to the common dc-link of the MMC as shown in Fig. 6(a), long battery strings are required negating most of the advantages of the cascaded structure, hence the distributed approach as shown in Fig. 6(b) represents the most feasible implementation of the MMC in energy storage applications.

A characteristic of the MMC topology is the presence of a circulating current within the phase-legs of the converter that provides additional freedom in dealing with SOC unbalances [47], [53], particularly for operation with grid imbalances [51]. However, benefits obtained by injection of circulating currents come at the cost of increased conduction and switching losses within the topology. Another problem is that dc-voltage injection in each converter arm results in a large fundamental frequency component appearing in the sub-module capacitor voltages, which then needs to be attenuated through the use of large submodule capacitors.

Further issues investigated in the literature for the use of MMC in BESS include the deployment of an integrated battery management system (BMS) based on SOC for the batteries in the converter [47], unbalances between the batteries that may lead to dc current injection to the grid [48] and, most importantly, the impact of low-order current harmonics that flow in the arms of the MMC on the batteries [18], [47]. The latter arises when batteries are directly connected to the dc-link of MMC SMs, resulting in low-order current harmonics flowing through the batteries.

When the MMC is considered solely for the purpose of connecting a BESS to the network, the additional complexity/cost of the MMC structure compared to a CHB (six arms instead of three), as well as the less optimal utilization of the converter (double the number of switching devices for the same number of voltage levels), put the MMC at a disadvantage as the topology of choice. However, integration of energy storage in MMC converters for HVDC transmission, motor drive systems or other grid support systems enhances the possible functions and the value which PE can provide in these applications [34], [52], [54], [55].

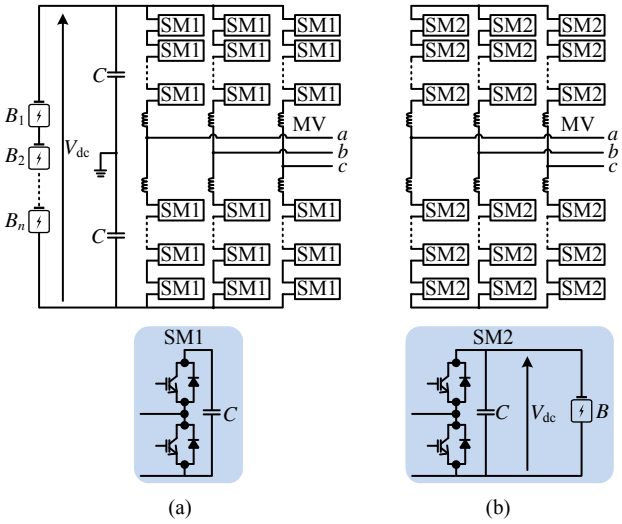


Fig. 6. Modular multilevel converter and corresponding submodules: (a) centralized batteries on the dc-link; (b) distributed batteries in the SMs.

## IV. Controllable Common dc-Link

A common characteristic of the previously presented PE configurations for BESS is that the converter dc-link voltage is directly defined by the voltage of the battery string. The battery voltages vary depending on the SOC, which introduces variation to the dc-link voltage. Grid-tied converters are required to accommodate the entire range of operating dc-voltage. Thus, their design in terms of semiconductor selection and operating points is not optimized. For instance, the voltage rating of semiconductor devices needs to be oversized to enable safe operation in the scenario of high SOC. In addition, the wide range of modulation indices to deal with the dc-voltage variation leads to decreased efficiency with higher ac output harmonics.

A controllable dc-link can be achieved by introducing an additional dc-dc conversion stage between the battery string and the dc-link of the grid-tied converters. In other words, the variations in the battery voltage are handled by the additional dc-dc converter, allowing optimized design of the grid-tied converter. An optimised design, based on dc-dc converters, that avoids overdimensioning of the batteries may also lead to a decrease of the total system cost, as less battery modules are required in the final system. Additionally, in the cascaded modular configurations presented in [18], [50], [51], the additional dc-dc converters between the SM and the battery can help eliminate the low-order harmonics flowing in the battery, and potentially increase battery lifetime. Certain dc-dc topologies

may also serve as protective and current limiting devices, eliminating the need for costly dc breakers.

In theory, any bidirectional dc-dc converter can be used to achieve control of the dc-link. However, step-up converters are normally considered in utility-scale BESS applications for the following reason. The grid connection voltage in MV applications is quite high with respect to the voltage of typical battery strings. Step-up converters also help reduce the required battery string voltages as well as the number of batteries in the string, thus potentially extending the life expectancy of batteries whose impedence is unavoidably slightly mismatched [56].

Several topologies for the bidirectional step-up dc-dc converter are proposed in the literature [57]–[61], two of which are presented in Fig. 7. The topology based on a simple boost converter, as shown in Fig. 7(a), is widely used owing to its simplicity. Another widely discussed topology is the dual-active-bridge (DAB ) [35], [58], [62]–[64], as shown in Fig. 7(b). This topology features galvanic isolation between the dc-link and the batteries owing to the use of a high-frequency isolation transformer, typically operating in the range of a few kHz (e.g. from 5 to 20 kHz). Consequently, the isolation transformer becomes relatively small and light, although transformer insulation ratings would need to withstand the complete phase-ground voltage if the batteries are grounded. The switching frequency of the converters can be increased with the use of Silicon Carbide (SiC) power devices. Furthermore, soft-switching techniques can be implemented to futher increase the converter efficiency [58]. The industrial standard for the isolation requirement in utility-scale battery applications is still being drafted [65], isolation may be necessary, as batteries are sensitive to over-current and temperature as a result of leakage current [56], [66].

High power, high current and high voltage are required in utility-scale BESS applications, where many long battery strings are connected in parallel. However, the impedance difference among strings leads to unbalanced charging, thus aging quickly and eventually damaging some of the strings. Moreover, in the modern battery industry, the battery pack including the short battery string has been already modularized [38], [39]. Therefore, it is expected that the PE unit will include a modular component to connect the battery packs as well as deal with the dc-voltage requirements. Instead of connecting batteries, modular dc-dc converters are connected in series and/or in parallel to comply with the power and voltage requirements. Regardless of the specific dc-dc topology, the connection configurations mainly have two categories: single input/output and multiple input/output [67]. Two multiple input/output configurations are presented in Fig. 8.

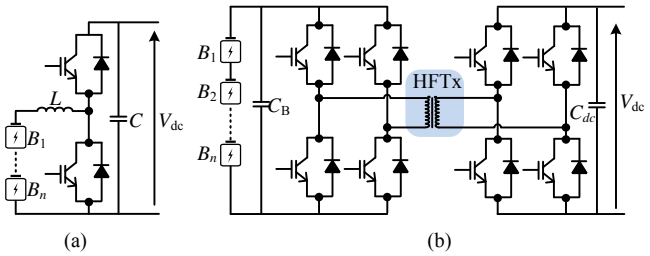


Fig. 7. Common dc-dc converter topologies to control the power flow between the common dc-link and batteries, (a) boost converter, and (b) dual active bridge converter.

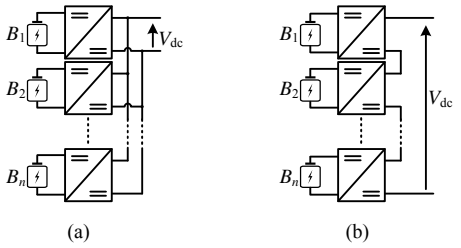


Fig. 8. Connection configurations of dc-dc converters suitable for multiple input/output, (a) parallel connection, and (b) series connection.

## V. Hybrid Energy Storage Systems

Hybrid energy storage systems (HESS) can combine the advantages of different energy storage (ES) technologies, such as specific power, energy density and cycling lifetime. In addition, the electrical characteristics of the combined technologies may be significantly different, e.g. cut-off voltage preventing overcharge. Therefore, a PE interface between different ES devices in the HESS is essential to control the terminal voltage as well as the power flow of each device.

Numerous configurations, connecting each ES device of the HESS to the common dc-link, have been proposed and discussed [17], [23], [68]–[74]. According to the controllability of the terminal voltage and power flow of each device, these topologies can be categorized into three groups: uncontrolled, semi-controlled, and fully-controlled, as shown in Fig. 9.

*a) Uncontrolled configuration:* The simplest configuration is illustrated in Fig. 9(a), where two ESs are connected in parallel directly to the common dc-link. In this configuration, the individual power flow of each ESs cannot be regulated. In addition, this configuration can only be used for ESs of similar voltage range, owing to lack of voltage control for individual terminals. Moreover, the ES voltage variation in different SOC leads to the voltage variation of each dc-link. In practice, an impedance is required between the ESs, in order to limit the surge current caused by voltage imbalances of the parallel-connected voltage sources. The need for the limiting impedance increases the losses of this configuration.

*b) Semi-controlled configuration:* A higher controllability can be achieved by connecting one of the ESs to the dc-link through a dc-dc converter, as shown in Fig. 9(b). This configuration also eliminates the need for current limiting impedances. The dc-dc converter can control the power flow and regulate the terminal voltage of $ES_1$ as different from the voltage of $ES_2$ and dc-link. However, voltage variation of the dc-link still exists due to variation in SOC of $ES_2$.

*c) Fully-controlled configuration:* The configuration presented in Fig. 9(c) provides full control of the terminal voltage and power flow for each ES device in the HESS. Each ES device connects to the common dc-link through a separate dc-dc converter, thus enabling voltage control of the dc-link.

TABLE I
MAJOR PE UNIT PROVIDERS FOR COMMISSIONED UTILITY BESS AND THEIR SOLUTIONS [9]

| PE Provider | Power/Energy (MW/MWh) | Topology | Battery Technology | dc-dc Stage | ac/dc Voltage (V) | Module Power Level |
|---|---|---|---|---|---|---|
| ABB | 20 / 6.67 | 2L/3L | Li-Ion | No | 415-690 $V_{ac}$; 975-1200 $V_{dc}$ | 72 kW - 1 MW |
| DynaPower | 11 / 4.4 | 2L/3L | Li-Ion | — | 750-1150 $V_{dc}$ | 1MVA |
| Enercon | 10 / 10 | 2L/3L | Li-Ion | Yes | — | 300 kW |
| Extreme Power | 10 / 7.5 | 2L | Advanced Lead Acid | — | 480 $V_{ac}$; 750-1200 $V_{dc}$ | 1.5MVA |
| General Electric | 21 / 14 | 2L/3L | Lead Acid | — | 480 $V_{ac}$; 431-850 $V_{dc}$ | 1.25 MW |
| Mitsubishi | 20 / 6.33 | 2L/3L | Li-Ion | — | 300 $V_{ac}$ | 0.5MW |
| Nidec | 12 / 96 | 2L | NaS | Yes | — | 1.2 - 2.5 MW |
| Parker SSD | 12 / 4 | 2L/3L | Li-Ion | No | 400-480 $V_{ac}$; 720-1200 $V_{dc}$ | 1.2 - 2.2 MW |
| S&C Electric | 10 / 0.14 | 2L/3L | Lead Acid | Yes | 480 $V_{ac}$; 460-800 $V_{dc}$ | 1 MW / 1.25 MVA |
| Younicos | 36 / 24 | 2L/3L | Advanced Lead Acid | — | 415-690 $V_{ac}$; 975-1200 $V_{dc}$ | 250 kVA |

— means manufacturer information not supplied

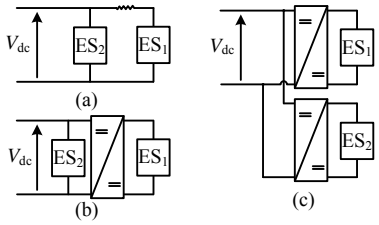


Fig. 9. Typical categories of configurations to connect multiple energy storage resources: (a) direct connected; (b) half controlled; and (c) fully controlled.

In addition, the dc-dc converters can individually regulate the terminal voltage of each device, i.e. the operation state of each device. To achieve these functions, many circuit topologies of the multi-port dc-dc converters have been proposed [75], [76] .

Integration of HESS can be deployed with some cascaded modular converters with existing PE devices. For instance, a typical HESS consisting of batteries and supercapacitors can be integrated by the MMC as presented in Fig. 6(a) where the batteries are connected to the dc-link and the supercapacitors are connected to submodules, or in Fig. 6(b) where the batteries and supercapacitors are connected to different submodules. The active power provided from the batteries/dc-link and the supercapacitors/submodules to the ac output can be regulated respectively by advanced control algorithms [77].

## VI. TOPOLOGY COMPARISON AND DISCUSSION

The aim of this section is to provide a comparison of the total power losses for configurations based on different PE topologies. The performance of these topologies is compared against a benchmark system, comprising of multiple parallel-connected, transformer-based 2L converters (Section II). Relative cost estimations are also provided.

### A. Major industrial solutions

A representative snapshot of existing utility-scale BESS installations is presented in Table I. The chosen industrial solutions in terms of PE topologies is that of 2L/3L converters. The transformer-based solution is currently favored by all PE providers, implying multiple converters connected on a common LV ac-grid to create large BESS systems.

It is worth noting that a 200 kWh pilot commissioned in Norfolk England in 2011 uses ABB's grid connected converter based on the series connection of semiconductors. The DynaPeaQ solution [78] from ABB is based on SVC Light technology and designed for applications up to 50 MW with only one monolithic converter. Use of series-connected press-pack IGBTs means transformer-less connection to the grid is possible.

### B. Candidate PE units and specifications

The benchmark BESS comprises 15 three-phase 2L converters and a line-frequency transformer. Four other configurations of PE units are compared to the benchmark for integrating a 30 MW battery energy storage system to a 22 kV electricity grid. In a configuration based on the 2L converter, 18 IGBTs are connected in series to block the dc-link of 36 kV, thus achieving direct integration to the 22 kV grid without the use of a transformer. Similarly, the 3L converter using series connection of semiconductors is also included in the comparison, where 9 IGBTs are connected in series. The remaining two selected configurations use the CHB and MMC converters, integrating batteries in each cell and submodule. Considering practical operation, a voltage safety factor is generally considered for redundancy, dynamics on capacitors and inductors, and low order harmonics for avoidance of over-modulation. For instance, in the 2L configuration, a factor of 1.4 is chosen to deal with redundancy and dynamics.

The detailed converter specifications of the selected five configurations, i.e. conventional 2L converter with transformer (2L+Tx), 2L/3L converter using series connected IGBTs, CHB and MMC, are provided in Table II.

In practical industrial solutions, various switching devices for different configurations would be used for optimization

TABLE II
SPECIFICATIONS OF SELECTED PE UNIT CONFIGURATIONS

| **Configuration** | **2L+Tx** | **2L** | **3L** | **CHB** | **MMC** |
|---|---|---|---|---|---|
| Three-phase Power | 30 MVA | | | | |
| Nominal Grid Voltage | 22 kV | | | | |
| # of Converters | 15 | 1 | 1 | 1 | 1 |
| # of cells / SMs | — | — | — | 10 | 40 |
| Transformer turn-ratio | 22/1.2 | — | — | — | — |
| $V_{acpeak}$ | 1.15 kV | 18 kV | | | |
| # IGBT in series | 1 | 18 | 9 | 1 | 1 |
| $V_{dc}, kV$ | 2.3 | 36 | 36 | 2.3 | 36 |
| Rated IGBT Voltage | 3.3 kV | | | | |
| IGBT cosmic-ray failure rate [80], [81] | 0.7 | | | | |
| Continuous dc collector current | 1 kA | | | | |
| Rated RMS Current | 825 A | 788 A | | | |
| Safety Factor | 1.3 | 1.4 | 1.4 | 1.5 | 1.5 |

TABLE III
CHARACTERISTICS OF SELECTED SEMICONDUCTOR [82]

| **Module: FZ1000R33HE3** | |
|---|---|
| Device type | IGBT |
| Collector-emitter voltage ($V_{CES}$) | 3300V |
| Continuous dc collector current ($I_{Cnom}$) | 1000A @ $T_C$=95°C & $T_{vjmax}$=150°C |
| Collector-emitter saturation voltage ($V_{CEsat}$) | Typ. 2.55V & Max. 3.1V @ $I_C$=1000A, $V_{GE}$=15V & $T_{vj}$=25°C |
| Device type | Diode |
| Repetitive peak reverse voltage ($V_{RRM}$) | 3300V |
| Continuous dc forward current ($I_F$) | 1000A |
| Forward Voltage ($V_F$) | Typ. 3.1V & Max. 3.85V @ $I_F$=1000A, $V_{GE}$=0V & $T_{vj}$=25°C |

purposes. However, for comparison purposes, the 3.3kV Infineon FZ1000R33HE3 is chosen in this paper for all five configurations. Compared to the 1.7 or 6.5 kV devices, the 3.3 kV range, of which the main characteristics are given in Table III, represents a good compromise between the higher switching power of high voltage devices and the lower cost of low voltage devices. It is also a good compromise between the high switching loss of high voltage devices and the high conduction loss associated with using a larger number of low voltage devices.

The same type of dc-dc converters, used to generate the controllable dc-link voltage is used in all configurations. In centralized battery configurations, the dc-dc converters are cascaded at the output forming a dc-link at tens of thousands volts, as presented in Fig. 8(b). In distributed battery configurations, the same number of converters is considered. In this paper, the estimated power losses of the DAB converter ($P_{\mathrm{dc-dc}}$) over various loading conditions are derived by considering the efficiency curves given by [63], [64]. In addition, the power loss of the step-up transformer ($P_{\mathrm{Tx}}$) is considered as 0.5% of the total power at full power [79].

### C. Loss calculation

The power loss of switching devices consists of the conduction and the switching loss [83], [84]. In the calculation of conduction losses, the IGBT is approximated by a constant voltage drop and a series resistance [83]. Then, the average conduction losses of IGBT ($P_{\mathrm{CT}}$) can be calculated by [83]:

$$P_{\mathrm{CT}} = V_{\mathrm{CE0}} \cdot \bar{I}_{\mathrm{T}} + R \cdot \tilde{I}_{\mathrm{T}}^2 \tag{1}$$

where $V_{\mathrm{CE0}}$ is the forward voltage drop at zero current, $R$ is the on-state resistance, $\bar{I}_{\mathrm{T}}$ and $\tilde{I}_{\mathrm{T}}$ are the average and rms current flowing through the IGBT. Both $V_{\mathrm{CE0}}$ and $R$ can be directly obtained from the IGBT datasheet.

Similarly, the average conduction losses of the anti-parallel diode ($P_{\mathrm{CD}}$) can be calculated by [83]:

$$P_{\mathrm{CD}} = V_{\mathrm{F0}} \cdot \bar{I}_{\mathrm{D}} + R' \cdot \tilde{I}_{\mathrm{D}}^2 \tag{2}$$

where $V_{\mathrm{F0}}$ and $R'$ can be read from the diode losses characteristics. Additionally, $\bar{I}_{\mathrm{D}}$ and $\tilde{I}_{\mathrm{D}}$ are the average and rms values of the current through the diode, respectively.

The switching losses, i.e. $P_{\mathrm{sw}}$ for IGBT and $P_{\mathrm{rec}}$ for diode, are calculated based on the turn-on and turn-off energy loss given in the datasheet. Neglecting parameter variations, the simplified value of the energy loss at different current levels can be obtained from the device datasheet. In this paper, the rms value of sinusoidal output current is used to decide the energy loss at all switching instants. It is worth noting that the switch-on losses in the diode are normally neglected [83]. Therefore, the losses of the IGBT ($P_{\mathrm{T}}$) and anti-parallel diode ($P_{\mathrm{D}}$) are given by:

$$P_{\mathrm{T}} = V_{\mathrm{CE0}} \cdot \bar{I}_{\mathrm{T}} + R \cdot \tilde{I}_{\mathrm{T}}^2 + \left[E_{\mathrm{on}}(\tilde{I}_T) + E_{\mathrm{off}}(\tilde{I}_T)\right] \cdot f_{\mathrm{sw}} \tag{3}$$

$$P_{\mathrm{D}} = V_{\mathrm{F0}} \cdot \bar{I}_{\mathrm{D}} + R' \cdot \tilde{I}_{\mathrm{D}}^2 + E_{\mathrm{rec}}(\tilde{I}_{\mathrm{D}}) \cdot f_{\mathrm{sw}} \tag{4}$$

where $f_{\mathrm{sw}}$ is the switching frequency. In this paper, the inverter losses do not include the losses of capacitors and inductors.

### D. Performance comparison and discussion

The average and rms currents through IGBTs and diodes are different for various PE configurations. The representations of current given in [83], [84] are used to calculate $P_{\mathrm{T}}$ and $P_{\mathrm{D}}$. The conversion efficiency is calculated by:

$$\eta = 1 - n \cdot (P_{\mathrm{T}} + P_{\mathrm{D}})/P_{\mathrm{total}} \tag{5}$$

where $n$ is the number of IGBTs or diodes and $P_{\mathrm{total}}$ is the total input power [85]. The power losses of the complete PE unit including the grid-tied converters, the additional dc-dc converters, and the step-up transformer are calculated and compared for various configurations.

Similarly, the conversion efficiencies of all PE units are presented as a function of the equivalent switching frequency and power level, as shown in Figs. 10 and 11, respectively. The efficiencies of configurations based on 2L converters decreases rapidly with the increase of switching frequency. Therefore,

these configurations should not operate at high switching frequency, as illustrated in dotted line in Fig. 10. The 3L converter based configuration has less efficiency drop against the increased switching frequency, and the configurations based on series connection of modular converters (i.e. CHB and MMC) provide the best efficiencies. This is because the actual switching frequencies of CHB and MMC are still low even at the equivalent 2L converter's switching frequency of 6kHz. Therefore, the quality of output sinusoidal waveform of CHB/MMC is better than other configurations, i.e. requiring smaller filters at the grid connection, this is one of the main advantages of the CHB/MMC.

The benchmark configuration using 2L transformer-based converters has the lowest efficiency at all power levels. In the configurations using series connection of semiconductors, the 3L converter has better performance than the 2L, by almost 1.5%. The configurations using either MMC or CHB provide the highest efficiency, which is approximately 3% higher compared to the benchmark system, while MMC has slightly higher efficiency than the CHB at heavy load.

The breakdown of power losses at two load levels provides further insight for the performance of different configurations, as presented in Fig. 12 and 13. The power level of 0.8 pu represents high load that is normally considered in power electronics design, and the power level of 0.1 pu represents the light load that can occur in some applications, e.g. smoothing the power output of RES [86]. The line-frequency transformer in the conventional configuration contributes a comparable amount of power loss with respect to the grid-tied converter. In other words, it justifies the incentive of using converters suitable for direct connection to the MV grid to remove the line-frequency transformer from the conversion system.

The additional dc-dc converters produce significant power losses, which to some extent explains why most industrial solutions currently do not include the additional dc-dc stage. Currently, there is a research gap in regards to the trade-off between the benefit from adding these dc-dc converters such as extending battery lifetime and the penalties of adding them such as lower efficiency and extra cost. Additionally, relevant standards that cover the use of dc-dc converters in utility-scale BESS applications are not available in the literature. Assuming the isolation function becomes the only reason for adding the dc-dc converters, the dc-dc converters can be removed from the benchmark configuration, as the step-up transformer is included. In this case, the power losses of CHB/MMC configurations are still slightly less than the losses of the conventional configuration. As expected, the loading conditions of the PE units not only affect the total power losses, but also change the proportion of each loss component, as shown in Fig. 12 and 13 for 80% and 10% load normalised to the full power, respectively.

It should be noted that the above loss evaluation and efficiency comparison corresponds to continuously operating PE units, for example in load-leveling, peak-shaving or intermittent renewable energy applications. In practice, many BESS will operate at no-load for an extended period of time (e.g. flicker mitigation, uninterruptible power supplies (UPS) etc). In these cases, the no-load losses of the system,

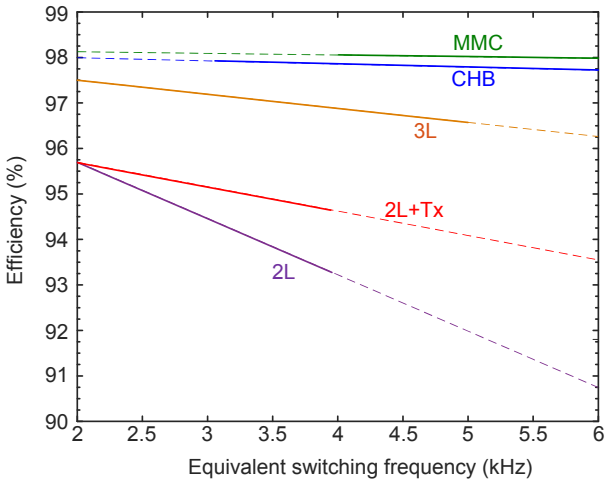


Fig. 10. Efficiency of compared configurations at various equivalent switching frequencies with the power level of 0.8 pu.

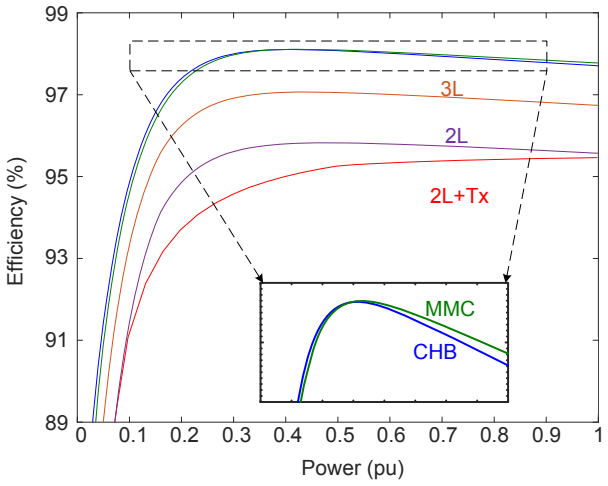


Fig. 11. Efficiency of compared configurations at various power levels.

predominantly the magnetisation losses of the transformer, become more important than the full-power losses. No-load losses are typically calculated on a per-application basis and define a loss-penalty cost for the operation of the BESS.

### *E. Cost and discussion*

The cost estimates on all compared configurations are presented in per-unit with respect to the cost estimate of the benchmark system, as shown in Fig. 14. Four major components, including the capacitors, silicon, filter, and transformer are considered in the calculation and comparison. The cost estimation for the benchmark system is based on detailed cost information provided from component manufacturers. All costs have been normalized based on a 30 MVA BESS application utilizing parallel-connected 2 MVA 2L converters with step-up transformer, similar to the analysis in [85] for solar PV systems.

Differences in the required capacitances for each configuration have been calculated based on [87]–[89] which provide

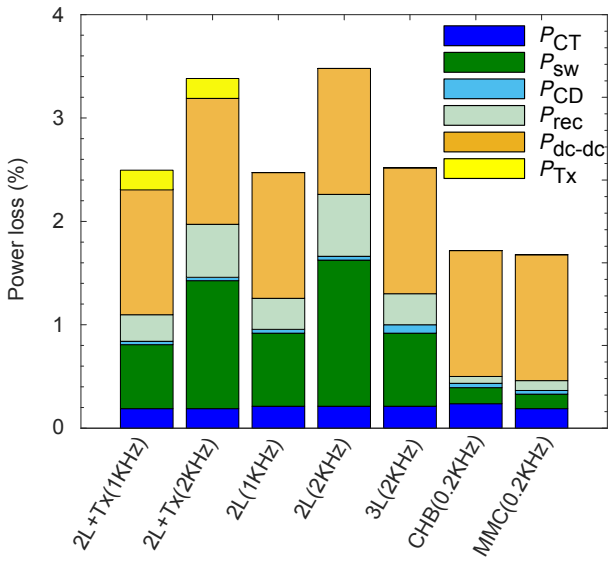


Fig. 12. Breakdown of entire PE unit losses for different configurations at 80% load.

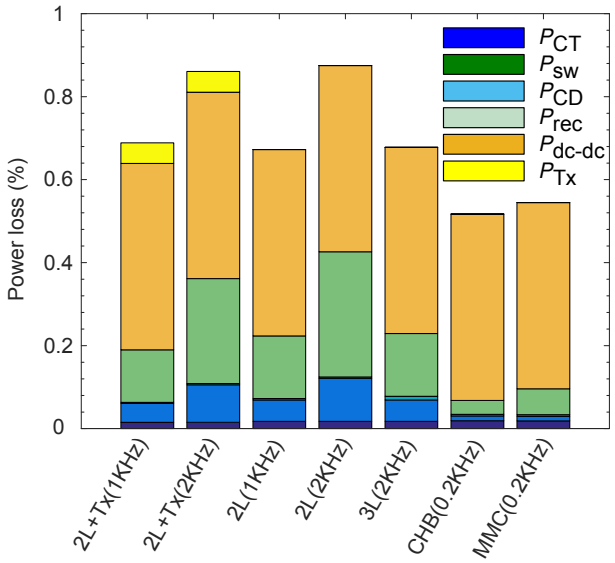


Fig. 13. Breakdown of entire PE unit losses for different configurations at 10% load.

capacitor sizing guidelines for the 3L, CHB and MMC converters respectively. Filter costs have been adjusted to ensure equal harmonic performance between all configurations. The difference in installed silicon power, and hence silicon cost, between configurations is calculated based on the number of semiconductors and their current ratings. The impact of no-load operation and annual load factor of the BESS has not been included as it applies on a case-by-case basis and cannot be easily generalised.

Overall, the CHB offers the lowest system cost comparative to other configurations. Comparing with the conventional configuration, the CHB saves the line-frequency transformer that contributes about 40% of the cost in the conventional configuration. Comparing with configuration using series connection of semiconductors, the CHB provides substantial savings on the filter at a cost of requiring larger capacitors. The MMC based configuration has the highest system cost, as it requires a significant amount of capacitance compared to others.

If the mechanical complexity is transferred to the system cost, the MMC-based configuration and others based on series connection of devices become even less competitive than the CHB-based configuration. If the size and weight of the components are transferred to the system cost, compared to the benchmark configuration, the CHB-based configuration with more capacitors can still be competitive as the bulky line-frequency transformer is removed. However, it is worth noting that the cost of the additional dc-dc converters is not included in the calculation, as we assume this cost is the same for all configurations. As mentioned previously, if dc-dc converters are required for isolation purposes only, their cost is only applicable to the CHB and MMC converters. As a result, the conventional configuration becomes more competitive, which also explains why the existing industrial solutions are mainly based on the conventional configuration.

The cost comparison performed in this paper has not considered the cost of protective devices or mechanical costs associated with the construction of each converter. More specifically, some of the salient protection/mechanical features of each topology are listed below:

- Topologies employing a series-connection of devices to create a high-voltage dc-link may require a high-voltage dc breaker to disconnect the batteries in case of a fault. In cascaded or parallel connected 2/3L converters typically less-costly low-voltage dc breakers can be utilised.
- Each cell in the cascaded topologies may require large dc capacitors to absorb second harmonic oscillations in instantaneous power produced by each phase-leg. Protection requirements are therefore increased due to the large amount of stored energy which is dissipated in the event of shoot-through of the dc-link. Depending on the battery technology, it may be feasible to absorb the second harmonic power oscillations within the batteries themselves, this way shoot-through currents would be inherently limited due to the internal impedance of the batteries.
- Parallel connected 2/3L converters can require large amounts of ac switchgear and bus bars, owing to the often multiple stages of aggregation that are required in stepping up the ac voltage by more than one order of magnitude.

In practice, these factors will also (along with the factors directly quantified in this paper) play a significant role in determining the most suitable BESS converter topology.

## VII. BESS Specific Issues and PE Topologies

One of the main functionalities of the PE unit in BESS application is to regulate the operating condition of batteries, as batteries are very sensitive to overcharge. Therefore, if the additional dc-dc converters are included to regulate the batteries, there is no apparent difference in terms of battery

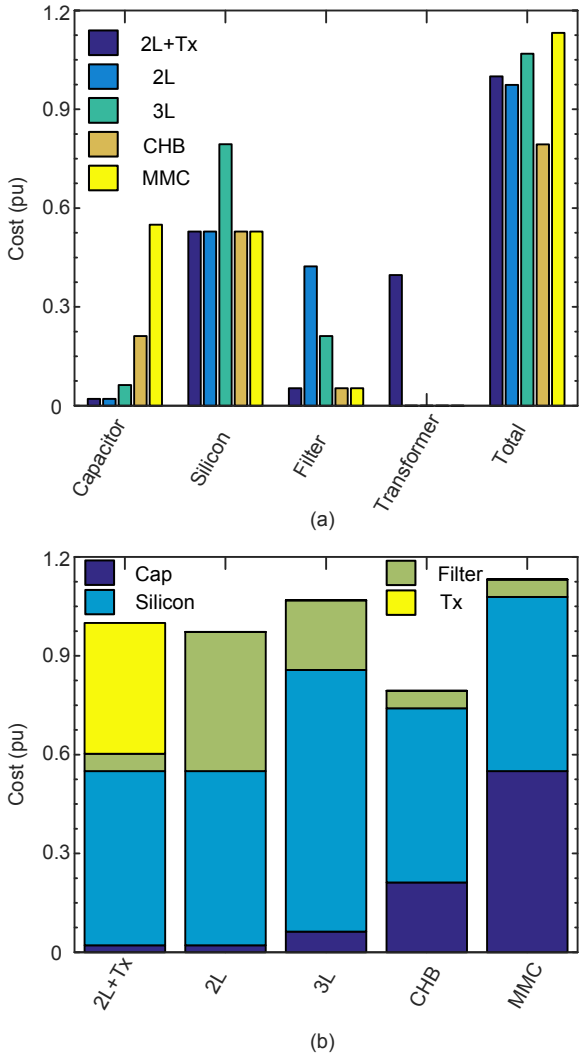


Fig. 14. Cost comparison for various configurations.

management and safety when using various grid-tied converters. If no dc-dc converters are considered, the low-order harmonics, for example occurring naturally in CHB/MMC or in other configurations under grid faults, may affect the battery life expectancy and even cause some safety concerns.

The relationship between low-order current harmonics and battery life for different battery technologies remains an open question in the literature at the time of writing. Some battery technologies, such as lithium-titanate [38], may have higher tolerance to low-order harmonics, and therefore be well suited for CHB/MMC applications employing no dc-dc conversion stage. However, the authors of this paper believe these relationships are influenced not only by battery technologies, but also on many external factors such as manufacturing processes, design of balancing circuits within battery modules and the stacking technique used to create the large system. For instance, the stacking technique can affect the heat distribution within each battery module. This means any lifetime degradation effect, due to additional heating generated by low order harmonics, will be highly dependent on, and possibly mitigated by, the stacking technique utilized.

Flow batteries are very different from other technologies in terms of system construction. The flow battery normally has complex mechanical components including the power stacks, the electrolyte tanks and circulating pipes. The capacity of individual battery system/module is normally larger than other battery technologies. Therefore, it can be difficult to distribute the flow battery in the CHB cells if the capacity of each cell is small.

In terms of grid support functionality, the CHB and MMC have some limitations during compensation of prolonged grid asymmetries. This is due to compensation of grid asymmetries implying unequal charge/discharge of batteries located in different phase-legs, which if allowed to persist can cause over/under-charge of the batteries. It has been noted in Section III that the MMC is more flexible in addressing SOC imbalances than the CHB. This is due to the possible utilisation of internal circulating currents, albeit at the cost of increased semiconductor losses. Nevertheless, transformer based solutions utilising 2/3L converters, where each phase-leg has a common dc-link, do not suffer from SOC imbalance during compensation of grid asymmetries. On the other hand, MMC and CHB solutions significantly reduce filtering requirements at the point of common coupling due to their superior waveform quality. From the viewpoint of the network operator, less filtering significantly reduces the possibility of creating unwanted resonances with the wider electrical network.

## VIII. Conclusion

This paper has provided a comparative review of commercially viable PE topologies suitable for utility-scale BESS applications. The efficiencies of entire PE units in various configurations have been compared and discussed. All transformerless configurations provide lower power losses than the conventional configuration at the cost of high mechanical complexity and more auxiliary devices.

Based on the provided analysis, the CHB based configuration provides the highest conversion efficiency along with the MMC based configuration. Moreover, if the additional dc-dc converters are not considered in the cost comparison, the CHB offers the lowest estimate of system cost. The requirement of including the additional dc-dc stage needs further investigation, as the dc-dc converters contribute significant losses to the entire PE conversion system. It also may make the CHB configuration less competitive to the conventional configuration using parallel connected 2L converters with the line-frequency step-up transformer.

In the future, the discussion and comparison may extend to other topologies available in the literature, such as cascaded modular push-pull converter [90], modular converter with series/parallel connectivity [91], and those integrated with the resonant concept [92]–[94], which are not included in this paper due to the lack of commercial viability with respect to the 2L and CHB-based configurations. Moreover, reconfigurable or multifunctional concepts should also be given attention [95], [96], as they have the potential to be a turning point in the future development of PE for BESS applications.

## REFERENCES


[1] International Energy Agency, "Trends 2015 in photovoltaic applications." [Online]. Available: http://www.iea-pvps.org/index.php?id=3

[2] Global Wind Energy Council, "Global wind report 2014: Annual market update." [Online]. Available: http://www.gwec.net/publications/global-wind-report-2/global-wind-report-2014-annual-market-update/

[3] CleanTechnica, "Renewables covered 80% of German electricity demand one afternoon last month." [Online]. Available: http://cleantechnica.com/2015/09/14/renewables-capable-of-covering-80-of-german-demand/

[4] GE Power, "GE signs its largest battery energy storage deal to date." [Online]. Available: https://www.genewsroom.com/press-releases/ge-signs-its-largest-battery-energy-storage-deal-date-281520

[5] T. DeVries, J. McDowall, N. Umbricht, and G. Linhofer, "Cold storage: The battery energy storage system for Golden Valley Electric Association," *ABB Review*, no. 1, pp. 38–43, 2004.

[6] V. Rudolf and K. D. Papastergiou, "Financial analysis of utility scale photovoltaic plants with battery energy storage," *Energy Policy*, vol. 63, pp. 139 – 146, 2013.

[7] AES, "AES to help SCE meet local power reliability with PPA for 100 MW of energy storage in California." [Online]. Available: http://www.aesenergystorage.com/2014/11/05/aes-help-sce-meet-local-power-reliability-20-year-power-purchase-agreement-energy-storage-california-new-facility-will-provide-100-mw-interconnected-storage-equivalent-200-mw/

[8] ——, "AES marks energy storage milestone with 400,000 MW-h of PJM service from Laurel Mountain." [Online]. Available: http://www.aesenergystorage.com/2013/04/11/aes-marks-energy-storage-milestone-with-400000-mw-h-of-pjm-service-from-laurel-mountain/

[9] US Department of Energy, "Global energy storage database." [Online]. Available: http://www.energystorageexchange.org/

[10] S. Vazquez, S. M. Lukic, E. Galvan, L. G. Franquelo, and J. M. Carrasco, "Energy storage systems for transport and grid applications," *IEEE Trans. Ind. Electron.*, vol. 57, no. 12, pp. 3881–3895, Dec 2010.

[11] M. Bragard, N. Soltau, S. Thomas, and R. W. De Doncker, "The balance of renewable sources and user demands in grids: Power electronics for modular battery energy storage systems," *IEEE Trans. Power Electron.*, vol. 25, no. 12, pp. 3049–3056, Dec 2010.

[12] B. M. Grainger, G. F. Reed, A. R. Sparacino, and P. T. Lewis, "Power electronics for grid-scale energy storage," *Proc. IEEE*, vol. 102, no. 6, pp. 1000–1013, June 2014.

[13] H. Akagi, "Large static converters for industry and utility applications," *Proc. IEEE*, vol. 89, no. 6, pp. 976–983, Jun 2001.

[14] C. Meyer, R. W. De Doncker, Y. W. Li, and F. Blaabjerg, "Optimized control strategy for a medium-voltage dvr - theoretical investigations and experimental results," *IEEE Trans. Power Electron.*, vol. 23, no. 6, pp. 2746–2754, Nov 2008.

[15] A. Chakraborty, S. K. Musunuri, A. K. Srivastava, and A. K. Kondabathini, "Integrating statcom and battery energy storage system for power system transient stability: a review and application," *Advances in Power Electronics*, vol. 2012, 2012.

[16] F. Daz-Gonzlez, A. Sumper, O. Gomis-Bellmunt, and R. Villaffila-Robles, "A review of energy storage technologies for wind power applications," *Renewable and Sustainable Energy Reviews*, vol. 16, no. 4, pp. 2154 – 2171, 2012. [Online]. Available: http://www.sciencedirect.com/science/article/pii/S1364032112000305

[17] X. Tan, Q. Li, and H. Wang, "Advances and trends of energy storage technology in microgrid," *International Journal of Electrical Power and Energy Systems*, vol. 44, no. 1, pp. 179 – 191, 2013. [Online]. Available: http://www.sciencedirect.com/science/article/pii/S0142061512003754

[18] I. Trintis, S. Munk-Nielsen, and R. Teodorescu, "A new modular multilevel converter with integrated energy storage," in *Proc. IEEE–IECON Conf.*, Nov 2011, pp. 1075–1080.

[19] L. Maharjan, S. Inoue, and H. Akagi, "A transformerless energy storage system based on a cascade multilevel pwm converter with star configuration," *IEEE Trans. Ind. Appl.*, vol. 44, no. 5, pp. 1621–1630, Sept 2008.

[20] L. Maharjan, T. Yamagishi, H. Akagi, and J. Asakura, "Fault-tolerant operation of a battery-energy-storage system based on a multilevel cascade pwm converter with star configuration," *IEEE Trans. Power Electron.*, vol. 25, no. 9, pp. 2386–2396, Sept 2010.

[21] Z. Zheng, K. Wang, L. Peng, Y. Li, and L. Xu, "A hybrid cascaded multi-level converter for power storage system," in *Proc. IEEE–EPE Conf.*, Sept 2013, pp. 1–10.

[22] S. D. G. Jayasinghe, D. M. Vilathgamuwa, and U. K. Madawala, "A new method of interfacing battery/supercapacitor energy storage systems for distributed energy sources," in *Proc. IEEE–IPEC Conf.*, Oct 2010, pp. 1211–1216.

[23] A. Etxeberria, I. Vechiu, S. Baudoin, H. Camblong, and J. Vinassa, "Control of a hybrid energy storage system using a three level neutral point clamped converter," in *Proc. IEEE–IECON Conf.*, Oct 2012, pp. 3400–3405.

[24] I. Trintis, "Grid converters for stationary battery energy storage systems," Ph.D. dissertation, Aalborg University, The Faculty of Engineering and Science, 2011.

[25] S. D. G. Jayasinghe and D. M. Vilathgamuwa, "Flying supercapacitors as power smoothing elements in wind generation," *IEEE Trans. Ind. Electron.*, vol. 60, no. 7, pp. 2909–2918, July 2013.

[26] H. S. Krishnamoorthy, D. Rana, and P. N. Enjeti, "A new wind turbine generator / battery energy storage utility interface converter topology with medium-frequency transformer," in *Proc. IEEE–APEC Conf.*, March 2013, pp. 2218–2224.

[27] S. D. G. Jayasinghe, D. M. Vilathgamuwa, and U. K. Madawala, "A battery energy storage interface for wind power systems with the use of grid side inverter," in *Proc. IEEE–ECCE Conf.*, Sept 2010, pp. 3786–3791.

[28] S. Burusteta, J. Pou, S. Ceballos Recio, I. Marino, J. A. Anzola, and V. G. Agelidis, "Capacitor voltage balancing in a three-level-converter-based energy storage system," *EPE Journal*, vol. 23, no. 4, Oct-Dec 2013.

[29] L. M. Grzesiak and J. G. Tomasik, "Autonomous power generating system with multi-level converters," in *Proc. IEEE–IECON Conf.*, Nov 2006, pp. 2815–2820.

[30] Y. Cheng, C. Qian, M. L. Crow, S. Pekarek, and S. Atcitty, "A comparison of diode-clamped and cascaded multilevel converters for a STATCOM with energy storage," *IEEE Trans. Ind. Electron.*, vol. 53, no. 5, pp. 1512–1521, Oct 2006.

[31] Y. Cheng and M. L. Crow, "A diode-clamped multi-level inverter for the StatCom/BESS," in *IEEE Power Engineering Society Winter Meeting*, vol. 1, 2002, pp. 470–475 vol.1.

[32] J. Pou, R. Pindado, D. Boroyevich, and P. Rodriguez, "Evaluation of the low-frequency neutral-point voltage oscillations in the three-level inverter," *IEEE Trans. Ind. Electron.*, vol. 52, no. 6, pp. 1582–1588, Dec 2005.

[33] P. Barbosa, P. Steimer, J. Steinke, M. Winkelnkemper, and N. Celanovic, "Active-neutral-point-clamped (ANPC) multilevel converter technology," in *EPE*, Sept 2005, pp. 10 pp.–P.10.

[34] H. Akagi, "Classification, terminology, and application of the modular multilevel cascade converter (mmcc)," *IEEE Trans. Power Electron.*, vol. 26, no. 11, pp. 3119–3130, Nov 2011.

[35] S. Thomas, M. Stieneker, and R. W. De Doncker, "Development of a modular high-power converter system for battery energy storage systems," in *Proc. IEEE–EPE Conf.*, Aug 2011, pp. 1–10.

[36] M. Stieneker, S. P. Engel, H. Stagge, and R. W. De Doncker, "Optimization of the pulse-width-modulation strategy for redundant and non-redundant multi-level cascaded-cell converters," in *Proc. IEEE–ECCE Conf.*, Sept 2013, pp. 101–108.

[37] L. Maharjan, T. Yamagishi, and H. Akagi, "Active-power control of individual converter cells for a battery energy storage system based on a multilevel cascade pwm converter," *IEEE Trans. Power Electron.*, vol. 27, no. 3, pp. 1099–1107, March 2012.

[38] N. Kawakami, S. Ota, H. Kon, S. Konno, H. Akagi, H. Kobayashi, and N. Okada, "Development of a 500-kw modular multilevel cascade converter for battery energy storage systems," *IEEE Trans. Ind. Appl.*, vol. 50, no. 6, pp. 3902–3910, Nov 2014.

[39] J. I. Y. Ota, T. Sato, and H. Akagi, "Enhancement of performance, availability, and flexibility of a battery energy storage system based on a modular multilevel cascaded converter (mmcc-ssbc)," *IEEE Trans. Power Electron.*, vol. 31, no. 4, pp. 2791–2799, April 2016.

[40] C. D. Townsend, T. J. Summers, and R. E. Betz, "Control and modulation scheme for a cascaded h-bridge multi-level converter in large scale photovoltaic systems," in *ECCE*, Sept 2012, pp. 3707–3714.

[41] M. Hagiwara, R. Maeda, and H. Akagi, "Negative-sequence reactive-power control by a PWM STATCOM based on a modular multilevel cascade converter (MMCC-SDBC)," *IEEE Trans. Ind. Appl.*, vol. 48, no. 2, pp. 720–729, March 2012.

[42] Y. Yu, G. Konstantinou, B. Hredzak, and V. G. Agelidis, "Power balance of cascaded h-bridge multilevel converters for large-scale photovoltaic integration," *IEEE Trans. Power Electron.*, vol. 31, no. 1, pp. 292–303, Jan 2016.

[43] T. J. Summers, R. E. Betz, and G. Mirzaeva, "Phase leg voltage balancing of a cascaded h-bridge converter based statcom using zero sequence injection," in *Proc. IEEE–EPE Conf.*, Sept 2009, pp. 1–10.

[44] L. Maharjan, S. Inoue, H. Akagi, and J. Asakura, "State-of-charge (soc)-balancing control of a battery energy storage system based on a cascade pwm converter," *IEEE Trans. Power Electron.*, vol. 24, no. 6, pp. 1628–1636, June 2009.

[45] P. Chanhom, S. Sirisukprasert, and N. Hatti, "Dc-link voltage optimization for soc balancing control of a battery energy storage system based on a 7-level cascaded pwm converter," in *International Conference on Electrical Engineering/Electronics, Computer, Telecommunications and Information Technology (ECTI-CON)*, May 2012, pp. 1–4.

[46] A. Hillers and J. Biela, "Optimal design of the modular multilevel converter for an energy storage system based on split batteries," in *Proc. IEEE–EPE Conf.*, Sept 2013, pp. 1–11.

[47] M. Schroeder, S. Henninger, J. Jaeger, A. Ras, H. Rubenbauer, and H. Leu, "Integration of batteries into a modular multilevel converter," in *Proc. IEEE–EPE Conf.*, Sept 2013, pp. 1–12.

[48] F. Gao, L. Zhang, Q. Zhou, M. Chen, T. Xu, and S. Hu, "State-of-charge balancing control strategy of battery energy storage system based on modular multilevel converter," in *Proc. IEEE–ECCE Conf.*, Sept 2014, pp. 2567–2574.

[49] A. Lachichi, "Modular multilevel converters with integrated batteries energy storage," in *International Conference on Renewable Energy Research and Application*, Oct 2014, pp. 828–832.

[50] T. Soong and P. W. Lehn, "Evaluation of emerging modular multilevel converters for bess applications," *IEEE Trans. Power Del.*, vol. 29, no. 5, pp. 2086–2094, Oct 2014.

[51] M. Vasiladiotis, N. Cherix, and A. Rufer, "Impact of grid asymmetries on the operation and capacitive energy storage design of modular multilevel converters," *IEEE Trans. Ind. Electron.*, vol. 62, no. 11, pp. 6697–6707, Nov 2015.

[52] M. A. Perez, S. Bernet, J. Rodriguez, S. Kouro, and R. Lizana, "Circuit topologies, modeling, control schemes, and applications of modular multilevel converters," *IEEE Trans. Power Electron.*, vol. 30, no. 1, pp. 4–17, Jan 2015.

[53] M. Vasiladiotis and A. Rufer, "Analysis and control of modular multilevel converters with integrated battery energy storage," *IEEE Trans. Power Electron.*, vol. 30, no. 1, pp. 163–175, Jan 2015.

[54] T. Jimichi, H. Fujita, and H. Akagi, "Design and experimentation of a dynamic voltage restorer capable of significantly reducing an energy-storage element," *IEEE Trans. Ind. Appl.*, vol. 44, no. 3, pp. 817–825, May 2008.

[55] S. P. Engel, M. Stieneker, N. Soltau, S. Rabiee, H. Stagge, and R. W. De Doncker, "Comparison of the modular multilevel dc converter and the dual-active bridge converter for power conversion in hvdc and mvdc grids," *IEEE Trans. Power Electron.*, vol. 30, no. 1, pp. 124–137, Jan 2015.

[56] S. T. Hung, D. C. Hopkins, and C. R. Mosling, "Extension of battery life via charge equalization control," *IEEE Trans. Ind. Electron.*, vol. 40, no. 1, pp. 96–104, Feb 1993.

[57] S. Waffler and J. W. Kolar, "A novel low-loss modulation strategy for high-power bidirectional buck + boost converters," *IEEE Trans. Power Electron.*, vol. 24, no. 6, pp. 1589–1599, June 2009.

[58] S. Inoue and H. Akagi, "A bidirectional dc-dc converter for an energy storage system with galvanic isolation," *IEEE Trans. Power Electron.*, vol. 22, no. 6, pp. 2299–2306, Nov 2007.

[59] R. W. De Doncker, D. M. Divan, and M. H. Kheraluwala, "A three-phase soft-switched high-power-density dc/dc converter for high-power applications," *IEEE Trans. Ind. Appl.*, vol. 27, no. 1, pp. 63–73, Jan 1991.

[60] T.-F. Wu, Y.-C. Chen, J.-G. Yang, and C.-L. Kuo, "Isolated bidirectional full-bridge dc-dc converter with a flyback snubber," *IEEE Trans. Power Electron.*, vol. 25, no. 7, pp. 1915–1922, July 2010.

[61] H. R. Karshenas, A. Bakhshai, A. Safaee, H. Daneshpajooh, and P. Jain, *Bidirectional dc-dc converters for energy storage systems*. INTECH Open Access Publisher, 2011.

[62] J. Everts, F. Krismer, J. Van den Keybus, J. Driesen, and J. W. Kolar, "Optimal zvs modulation of single-phase single-stage bidirectional dab ac-dc converters," *IEEE Trans. Power Electron.*, vol. 29, no. 8, pp. 3954–3970, Aug 2014.

[63] C. Gammeter, F. Krismer, and J. W. Kolar, "Comprehensive conceptualization, design, and experimental verification of a weight-optimized all-sic 2kv/700v dab for an airborne wind turbine," *IEEE Journal of Emerging and Selected Topics in Power Electronics*, vol. PP, no. 99, pp. 1–1, 2015.

[64] H. Akagi, T. Yamagishi, N. M. L. Tan, S.-I. Kinouchi, Y. Miyazaki, and M. Koyama, "Power-loss breakdown of a 750-v 100-kw 20-khz bidirectional isolated dc-dc converter using sic-mosfet/sbd dual modules," *IEEE Trans. Ind. Appl.*, vol. 51, no. 1, pp. 420–428, Jan 2015.

[65] IEEE Standards Association, "Standard for the design of battery chargers used in stationary applications." [Online]. Available: https://standards.ieee.org/develop/project/2405.html

[66] W. F. Bentley, "Cell balancing considerations for lithium-ion battery systems," in *Battery Conference on Applications and Advances*, Jan 1997, pp. 223–226.

[67] R. Ayyanar, R. Giri, and N. Mohan, "Active input-voltage and load-current sharing in input-series and output-parallel connected modular dc-dc converters using dynamic input-voltage reference scheme," *IEEE Trans. Power Electron.*, vol. 19, no. 6, pp. 1462–1473, Nov 2004.

[68] A. Etxeberria, I. Vechiu, H. Camblong, and J.-M. Vinassa, "Comparison of three topologies and controls of a hybrid energy storage system for microgrids," *Energy Conversion and Management*, vol. 54, no. 1, pp. 113 – 121, 2012. [Online]. Available: http://www.sciencedirect.com/science/article/pii/S0196890411002779

[69] S. Lemofouet and A. Rufer, "A hybrid energy storage system based on compressed air and supercapacitors with maximum efficiency point tracking (MEPT)," *IEEE Trans. Ind. Electron.*, vol. 53, no. 4, pp. 1105–1115, June 2006.

[70] W. Li and G. Joos, "A power electronic interface for a battery supercapacitor hybrid energy storage system for wind applications," in *Proc. IEEE–PESC Conf.*, June 2008, pp. 1762–1768.

[71] R. A. Dougal, S. Liu, and R. E. White, "Power and life extension of battery-ultracapacitor hybrids," *IEEE Trans. Comp. Packag. Technol.*, vol. 25, no. 1, pp. 120–131, Mar 2002.

[72] C. Abbey, K. Strunz, and G. Joos, "A knowledge-based approach for control of two-level energy storage for wind energy systems," *IEEE Trans. Energy Convers.*, vol. 24, no. 2, pp. 539–547, June 2009.

[73] L. Gao, R. A. Dougal, and S. Liu, "Power enhancement of an actively controlled battery/ultracapacitor hybrid," *IEEE Trans. Power Electron.*, vol. 20, no. 1, pp. 236–243, Jan 2005.

[74] S. Pay and Y. Baghzouz, "Effectiveness of battery-supercapacitor combination in electric vehicles," in *IEEE Power Tech Conference Proceedings*, vol. 3, June 2003, pp. 6 pp. Vol.3–.

[75] H. Tao, J. L. Duarte, and M. A. M. Hendrix, "Three-port triple-half-bridge bidirectional converter with zero-voltage switching," *IEEE Trans. Power Electron.*, vol. 23, no. 2, pp. 782–792, March 2008.

[76] Y.-M. Chen, Y.-C. Liu, and S.-H. Lin, "Double-input PWM dc/dc converter for high-/low-voltage sources," *IEEE Trans. Ind. Electron.*, vol. 53, no. 5, pp. 1538–1545, Oct 2006.

[77] F. Guo and R. Sharma, "A modular multilevel converter with half-bridge submodules for hybrid energy storage systems integrating battery and ultracapacitor," in *Proc. IEEE–APEC Conf.*, March 2015, pp. 3025–3030.

[78] ABB, "DynaPeaQ SVC Light with energy storage." [Online]. Available: http://www02.abb.com/global/gad/gad02181.nsf/0/1c9442cf6083140ac1257a62003621b

[79] Siemens, "Power transformers - machine and network transformers from 30 to over 1300 MVA." [Online]. Available: http://www.energy.siemens.com/br/en/power-transmission/transformers/power-transformers/medium-power-transformers.htm

[80] F. Bauer, N. Kaminski, S. Linder, and H. Zeller, "A high voltage igbt and diode chip set designed for the 2.8 kV dc link level with short circuit capability extending to the maximum blocking voltage," in *International Symposium on Power Semiconductor Devices and ICs*, 2000, pp. 29–32.

[81] T. Shoji, S. Nishida, T. Ohnishi, T. Fujikawa, N. Nose, M. Ishiko, and K. Hamada, "Neutron induced single-event burnout of IGBT," in *Proc. IEEE–IPEC Conf.*, June 2010, pp. 142–148.

[82] Infineon, "FZ1000R33HE3 data sheet." [Online]. Available: https://www.infineon.com/cms/en/product/

[83] D. Graovac and M. Purschel, "Igbt power losses calculation using the data-sheet parameters-application note," 2009.

[84] G. I. Orfanoudakis, S. M. Sharkh, M. A. Yuratich, and M. A. Abusara, "Loss comparison of two and three-level inverter topologies," in *IET-PEMD*, April 2010, pp. 1–6.

[85] J. Sastry, P. Bakas, H. Kim, L. Wang, and A. Marinopoulos, "Evaluation of cascaded h-bridge inverter for utility-scale photovoltaic systems," *Renewable Energy*, vol. 69, pp. 208 – 218, 2014. [Online]. Available: http://www.sciencedirect.com/science/article/pii/S0960148114002134

[86] G. Wang, M. Ciobotaru, and V. G. Agelidis, "Power management for improved dispatch of utility-scale PV plants," *IEEE Trans. Power Syst.*, vol. PP, no. 99, pp. 1–10, 2015.

[87] M. Schweizer, T. Friedli, and J. W. Kolar, "Comparative evaluation of advanced three-phase three-level inverter/converter topologies against two-level systems," *IEEE Trans. Ind. Electron.*, vol. 60, no. 12, pp. 5515–5527, Dec 2013.

[88] D. Soto and T. C. Green, "A comparison of high-power converter topologies for the implementation of FACTS controllers," *IEEE Trans. Ind. Electron.*, vol. 49, no. 5, pp. 1072–1080, Oct 2002.

[89] L. Baruschka and A. Mertens, "Comparison of cascaded h-bridge and modular multilevel converters for bess application," in *Proc. IEEE–ECCE Conf.*, Sept 2011, pp. 909–916.

[90] M. Hagiwara and H. Akagi, "Experiment and simulation of a modular push-pull pwm converter for a battery energy storage system," *IEEE Trans. Ind. Appl.*, vol. 50, no. 2, pp. 1131–1140, March 2014.

[91] S. M. Goetz, A. V. Peterchev, and T. Weyh, "Modular multilevel converter with series and parallel module connectivity: Topology and control," *IEEE Trans. Power Electron.*, vol. 30, no. 1, pp. 203–215, Jan 2015.

[92] R. W. De Doncker and J. P. Lyons, "The auxiliary resonant commutated pole converter," in *IEEE Industry Applications Society Annual Meeting*, Oct 1990, pp. 1228–1235 vol.2.

[93] J. G. Cho, J. W. Baek, D. W. Yoo, and Y. W. Chung, "Three level auxiliary resonant commutated pole inverter for high power applications," in *Proc. IEEE–PESC Conf.*, vol. 2, Jun 1996, pp. 1019–1026 vol.2.

[94] C. Turpin, L. Deprez, F. Forest, F. Richardeau, and T. A. Meynard, "A ZVS imbricated cell multilevel inverter with auxiliary resonant commutated poles," *IEEE Trans. Power Electron.*, vol. 17, no. 6, pp. 874–882, Nov 2002.

[95] T. Kim, W. Qiao, and L. Qu, "Power electronics-enabled self-x multicell batteries: A design toward smart batteries," *IEEE Trans. Power Electron.*, vol. 27, no. 11, pp. 4723–4733, Nov 2012.

[96] I. Mazhari, M. Chamana, B. H. Chowdhury, and B. Parkhideh, "Distributed pv-battery architectures with reconfigurable power conversion units," in *Proc. IEEE–APEC Conf.*, March 2014, pp. 691–698.


**Guishi Wang** (S'10–M'16) received the B.Eng. degree in electrical engineering and automation from the Northwestern Polytechnic University, Xi'an, China, in 2007, and the Ph.D. degree in electrical engineering from the UNSW Australia (The University of New South Wales), Sydney, Australia, in 2015. Since 2014, he was a Research Associate with the Australian Energy Research Institute (AERI) and the School of Electrical Engineering and Telecommunications, UNSW Australia. His research interests included the hybrid energy storage system supporting the dispatch of large-scale renewable generations and the grid integration of large-scale battery system. Currently, he is with the Elite International Investment focusing on the sustainable property development.

**Georgios Konstantinou** (S'08–M'11) received the B.Eng. degree in electrical and computer engineering from the Aristotle University of Thessaloniki, Thessaloniki, Greece, in 2007 and the Ph.D. degree in electrical engineering from UNSW Australia, Sydney, in 2012. From 2012 to 2015 he was a Research Associate with the Australian Energy Research Institute at UNSW Australia. He is currently a Lecturer with the School of Electrical Engineering and Telecommunications at UNSW. His research interests include hybrid and modular multilevel converters, power electronics for HVDC and energy storage applications, pulse width modulation and selective harmonic elimination techniques for power electronics.

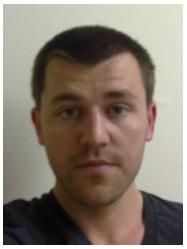

**Christopher D. Townsend** (S'09–M'13) received the B.E. (2009) and Ph.D. (2013) degrees in electrical engineering from the University of Newcastle, Australia. He was with ABB Corporate Research, Vsters, Sweden and The University of New South Wales, Australian Energy Research Institute, Sydney, Australia. He is currently with the School of Electrical Engineering and Computer Science, University of Newcastle, Australia. His current research interests include topologies and modulation strategies for multi-level converters. He is a member of the Power Electronics and Industrial Electronics Societies of the IEEE.

**Josep Pou** (S'97– M'03–SM'15) received the B.S., M.S., and Ph.D. degrees in electrical engineering from the Technical University of Catalonia (UPC) Barcelona-Tech, in 1989, 1996, and 2002, respectively.

In 1990, he joined the Faculty of UPC as an Assistant Professor, where he became an Associate Professor in 1993. From Feb. 2013 to Aug. 2016, he was a Professor with the University of New South Wales (UNSW), Sydney, Australia. Since Set. 2016, he has been an Associate Professor with the Nanyang Technological University (NTU), Singapore. In 2001 and 2006, he was a Researcher with the Center for Power Electronics Systems, Virginia Tech, Blacksburg, VA, USA. In 2012, he was a Researcher with the Australian Energy Research Institute, UNSW. Since 2006, he has collaborated with TECNALIA Research and Innovation as a Research Consultant. His current research interests include modulation and control of power converters, multilevel converters, renewable energy generation, energy storage, power quality, and high voltage dc transmission systems. He has authored over 200 published technical papers, and has been involved in several industrial projects and educational programs in the fields of power electronics and systems.

**Sergio Vazquez** (S'04–M'08) was born in Seville, Spain, in 1974. He received the B.S, M.S. and PhD degrees in industrial engineering from the University of Seville (US) in 2003, 2006, and 2010, respectively. In 2002, he was with the Power Electronics Group, US, working in R&D projects. He is currently an Associate Professor with the Department of Electronic Engineering, US. His research interests include power electronics systems, modeling, modulation and control of power electronics converters applied to renewable energy technologies.

Dr. Vazquez was recipient as coauthor of the 2012 Best Paper Award of the IEEE Transactions on Industrial Electronics.

**Dr. Georgios D. Demetriades** was born in Famagusta Cyprus. He received his M.Sc. degree in Electrical Engineering at the Democritus University of Thrace in Greece, his Technical Licentiate degree and his Ph.D degree both in Power Electronics from the Royal Institute of Technology, KTH, in Stockholm, Sweden. He worked in Cyprus for a two years period and in 1995 he joined what is today known as ALSTOM Power Environmental Systems in Sweden. In the year 2000 he joined ABB Corporate Research where he is currently working as a research and development manager. From 2013 he is a visiting associated professor in the Indian Institute of Technology, IIT Bombay, Mumbai, India. His main research interests include power electronics, VSC HVDC, FACTS devices, high-frequency DC-DC power resonant converters and high-frequency electromagnetic modeling.

**Vassilios G. Agelidis** (SM'00 - F'16) was born in Serres, Greece. He received the B.Eng. degree in electrical engineering from the Democritus University of Thrace, Thrace, Greece, in 1988; the M.S. degree in applied science from Concordia University, Montreal, QC, Canada, in 1992; and the Ph.D. degree in electrical engineering from Curtin University, Perth, Australia, in 1997.

From 1993 to 1999, he was with the School of Electrical and Computer Engineering, Curtin University of Technology. In 2000, he joined the University of Glasgow, Glasgow, U.K., as a Research Manager for the Glasgow-Strathclyde Center for Economic Renewable Power Delivery. From 2005 to 2006, he was the Inaugural Chair of Power Engineering with the School of Electrical, Energy, and Process Engineering, Murdoch University, Perth. From 2006 to 2010, he was the Energy Australia Chair of Power Engineering with the University of Sydney, Sydney, NSW, Australia. He is currently the Director of the Australian Energy Research Institute, UNSW Australia, Sydney. He has authored/co-authored several journal and conference papers, as well as Power Electronic Control in Electrical Systems.